Publ. Astron. Soc. Japan **42**, 249–267 (1990)

Hydrodynamical Winds from an Accretion Disk

Jun FUKUE and Rika OKADA*

Astronomical Institute, Osaka Kyoiku University, Tennoji-ku, Osaka 543

(Received 1989 January 6; accepted 1989 October 13)

Abstract

It is expected that hot gas emanates hydrodynamically from the surface of an accretion disk in the gravitational field of a central object through internal heating or irradiation. We examine such disk winds under a simple approximation in which the force balances parallel and perpendicular to the streamlines are decoupled. The angular momentum is assumed to be conserved along each streamline. The energy is injected into each streamline at the flow base on the surface of the disk. Under these approximations, we reveal the properties of a two-dimensional flow pattern, such as the transonic surfaces, of disk winds. When the temperature distribution at the wind base is not so steep (flatter than $1/r_e$, r_e being the equatorial distance), the gas of the inner disk is gravitationally bound near the disk to form a corona, while the gas on the outer disk is unbound to escape infinity, passing through the critical points. On the other hand, if the temperature distribution is steeper than $1/r_e$, the gas on the inner disk is unbound and that on the outer disk is bound. When it is $1/r_e$, the gas is free or bound all over the disk surface. Although the transonic nature, such as the location or number of the critical points, depends naively on the configuration of streamlines, the global behavior is independent of the streamlines and shows the characteristic properties of hydrodynamical winds from the disk.

Key words: Accretion disks; Astrophysical jets; Critical points; Winds.

1. Introduction

An accretion disk is a promising engine of various active astronomical phenomena: e.g., active galactic nuclei (AGN), binary X-ray sources, SS 433, star-forming regions, and so on. So far, the structures of disks have been extensively studied. Toward the "bi-decennial" of an accretion disk after Lynden-Bell (1969), attention is presently being focused on the interaction between the disk and such circumstances as the photon spectra, matter ejection, and influence through the magnetic field.

*Present address: Department of Physics, Tokyo Metropolitan University, Setagaya-ku, Tokyo 158.

Of these, mass outflow from the disk is important in relation to astrophysical jets. Many researchers have investigated steady flows from geometrically thin disks (Meier 1979, 1982; Katz 1980; Begelman et al. 1983; Begelman and McKee 1983; Fukue 1989; Blandford and Payne 1982; Sakurai 1987), and those in the funnel of the astrophysical torus (Fukue 1982, 1983; Calvani and Nobili 1983; Ferrari et al. 1984; Eggum et al. 1985; Lu 1986; Chakrabarti 1986). In these studies, attention was mainly focused on the driving mechanisms through thermal, radiative, centrifugal, and magnetical processes.

In a previous paper (Fukue 1989, hereafter referred to as Paper I), Fukue examined the two-dimensional hydrodynamical winds from a disk, using a one-dimensional approximation in which the configuration of the streamlines of flow is given a priori. He obtained the locations of the critical points in the meridional plane and pointed out that the velocity fields become somewhat complicated in the wind from the disk. This is partly because the difference in the gravitational potential between the flow base and the infinity is finite, and mainly because the energy sources are distributed at the flow base. Moreover, he found that if the energy distribution on the disk is uniform, the gas in the inner region of the disk is gravitationally bound to form a corona, while the gas in outer disk escapes to infinity, passing through critical points.

In Paper I the treatment was restricted in the sense that the angular momentum of the flow is ignored and the streamlines are given a priori. Recently, Takahara et al. (1989) examined similar problems, using a simplified model in which the streamlines are determined by the radial balance between the gravitational force and the centrifugal force. In their model, however, the force balance perpendicular to the streamline was not treated properly. Furthermore, the two-dimensional behavior of the flow was not considered in their paper.

Thus in this paper we reexamine the hydrodynamical winds from a geometrically thin disk (*disk winds*), including the rotation of the gas. We decouple the force balances into perpendicular and parallel components to the streamline and solve each component self-consistently. We also demonstrate the two-dimensional global properties of disk winds which are similar to those without rotation (discussed in Paper I), although the location or the number of critical points depends on the configuration of the streamlines adopted.

In the next section the basic equations are presented. The configurations of the streamlines are derived in section 3. The disk winds are discussed in section 4. The final section is devoted to discussion. A simplified treatment of the streamline is described in the Appendix for a comparison.

2. Basic Equations

Let's consider a gas which is flowing out from the surface of a geometrically thin Keplerian disk surrounding a central object of mass m. The self-gravity of the disk is neglected. The flow is supposed to be steady and axisymmetric. It is further assumed that the gas flow is inviscid and polytropic. The magnetic field in the gas flow is ignored in this paper. Hence, the specific angular momentum of the gas is conserved along the streamline. We use cylindrical coordinates (r, ϕ, z) with the z-axis along the rotation axis of the disk. Therefore, the configuration of streamlines is given by

$r = r(z; r_e)$, where r_e is the radial distance of the base of the streamline on the disk. Each streamline is labeled by r_e, as in Paper I.

We treat the momentum equation as being the perpendicular component and the parallel component to the streamline, seperately. If the pressure gradient force perpendicular to the streamline is neglected, the force balance perpendicular to the streamline determines the configuration of streamlines $r = r(z; r_e)$, as below. The force balance parallel to the streamline gives the flow field of disk winds.

Using line element ds along the streamline and dn perpendicular to the streamline, we can express the equations of motion perpendicular and parallel to the streamline, respectively, as (cf. Paper I)

$$\frac{1}{\rho}\frac{dp}{dn} = -\frac{Gm}{(r^2+z^2)^{3/2}}\frac{rdz - zdr}{ds} + \frac{L^2}{r^3}\frac{dz}{ds} \tag{1}$$

and

$$v\frac{dv}{ds} + \frac{1}{\rho}\frac{dp}{ds} = -\frac{Gm}{(r^2+z^2)^{3/2}}\frac{rdr + zdz}{ds} + \frac{L^2}{r^3}\frac{dr}{ds}, \tag{2}$$

where ρ is the density, p the pressure, v the velocity along the streamline, and L the specific angular momentum.

As mentioned before, if we neglect the pressure gradient force in the force balance perpendicular to the streamline, equation (1) determines the configuration of streamlines,

$$\frac{Gm}{(r^2+z^2)^{3/2}}\left(r - z\frac{dr}{dz}\right) = \frac{L^2}{r^3}. \tag{3}$$

Furthermore, from equation (2), the momentum equation along the streamline becomes

$$v\frac{dv}{dz} + \frac{1}{\rho}\frac{dp}{dz} + \frac{d\phi}{dz} = 0, \tag{4}$$

where the force $-d\phi/dz$ along the streamline is expressed as

$$-\frac{d\phi}{dz} = -\frac{Gm}{(r^2+z^2)^{3/2}}\left(z + r\frac{dr}{dz}\right) + \frac{L^2}{r^3}\frac{dr}{dz}. \tag{5}$$

The first term on the right-hand side of equation (5) is the gravitational acceleration by the central object along the streamline, whereas the second term is the centrifugal force, which is newly included in the present analysis.

Along each streamline, the gas conserves its specific angular momentum which the gas has at the base on the surface of the disk. Since the disk rotation is Keplerian, the angular momentum conservation can be written as

$$L = (Gmr_e)^{1/2}, \tag{6}$$

where r_e is the radial distance of the flow base and specifies each streamline (as was noted).

The continuity equation along each streamline is

$$A\rho v = \dot{M}_{\rm e} \ (\text{constant}), \tag{7}$$

where the mass effluxion rate $\dot{M}_{\rm e}$ is generally a function of the streamline. The cross-sectional area A of the flow is given by

$$A = \left[1 + \left(\frac{dr}{dz}\right)^2\right]^{-1/2} \left.\frac{2\pi r \partial r}{2\pi r_{\rm e} \partial r_{\rm e}}\right|_{\rm z}, \tag{8}$$

where $2\pi r \partial r / 2\pi r_{\rm e} \partial r_{\rm e}|_{\rm z}$ is the change in the horizontal area along the streamline, and $[1 + (dr/dz)^2]^{-1/2}$ is the projection factor.

Finally, the polytropic relation is adopted:

$$p/\rho^{\gamma} = K_{\rm e} \ (\text{constant}). \tag{9}$$

Here, γ is a constant and $K_{\rm e}$ is the streamline-function.

Integrating equation (4) under angular momentum conservation (6), we obtain the Bernoulli equation along the streamline,

$$\frac{v^2}{2} + \frac{c^2}{\gamma - 1} + \phi = E_{\rm e} \ (\text{constant}), \tag{10}$$

where $c^2 = \gamma p/\rho$ is the square of the sound speed. In equation (10), the effective potential ϕ is determined so that it vanishes at the base of each streamline. Therefore, it is expressed as

$$\phi = -\frac{Gm}{(r^2 + z^2)^{1/2}} + \frac{Gm}{r_{\rm e}} + \frac{L^2}{2}\left(\frac{1}{r^2} - \frac{1}{r_{\rm e}^2}\right). \tag{11}$$

In this equation the first two terms on the right-hand side express the gravitational potential and the third term is the centrifugal potential.

Since for the wind considered here $v \ll c$ and $\phi = 0$ at the wind base, constant $E_{\rm e}$ in equation (10) indicates the enthalpy injected into the flow at the base of each streamline. For thermal winds, this constant reflects the temperature distribution $T_{\rm e}$ of the gas on the disk. Although $E_{\rm e}$ (or $T_{\rm e}$) is generally an arbitrary function of the streamline, we assume for simplicity that they can be expressed as a power of the radius $r_{\rm e}$ of the wind base, as in Paper I,

$$E_{\rm e} = \frac{\gamma}{\gamma - 1}\frac{\mathcal{R}}{\mu} T_{\rm e} \propto r_{\rm e}^{-q}, \tag{12}$$

where $\mathcal{R}$ is the gas constant, μ the mean molecular weight, and q a constant.

Equations (6), (7), (9), and (10) are then the basic equations in integration forms governing the flow structure along the streamline determined by equation (3).

After manipulating the basic equations above, we have a single ordinary differential equation, the so-called wind equation. In terms of the Mach number ($M = v/c$), the wind equation can be written

$$dM^2/dz = N/D, \tag{13}$$

where

$$D = M^2 - 1 \tag{14}$$

and

$$N = M^2[(\gamma-1)M^2+2]\left[\frac{A'}{A} - \frac{\gamma+1}{2(\gamma-1)}\frac{\phi'}{E_e-\phi}\right]. \tag{15}$$

In equation (15) the prime denotes differentiation with respect to z. Moreover, ϕ' and ϕ are, respectively, given by equations (5) and (11), and E_e is given by equation (12).

As is well-known, equation (13) has critical points where the denominator D and the numerator N vanish simultaneously. In the present case, the critical points are also transonic points where the Mach number becomes unity. Furthermore, when these critical points exist, the types of critical points are always saddle or center, since there are no dissipational processes in the present flow.

In the remainder of this paper, we take some reference radius r_0 and $(Gm/r_0)^{1/2}$ as the units of length and velocity, respectively. By using this normalization, the Bernoulli equation, e.g., can be rewritten as

$$\frac{v^2}{2} + \frac{c^2}{\gamma-1} + \phi = \frac{\gamma\varepsilon}{\gamma-1} r_e^{-q}, \tag{16}$$

where the unit of the normalized variables (v^2, c^2, and ϕ) is (Gm/r_0) and that of r_e is r_0. Furthermore, $\varepsilon = (\mathcal{R}/\mu)T_0/(Gm/r_0)$ is the ratio of the thermal energy to the gravitational energy at the reference radius r_0.

Under the semi-two-dimensional treatment presented here, the flow field is specified by radius r_e of the flow base on the surface of the disk. Hence, the parameters are ultimately γ, ε, and q.

3. The Configuration of Streamlines

In this paper we have assumed that gas is flowing out from the disk along a streamline determined by equation (3), meaning a balance between gravitational and centrifugal accelerations perpendicular to the streamline, itself.

With the help of angular momentum conservation (6) along the streamline, we rewrite equation (3) as

$$\frac{dr}{dz} = \frac{r - r_e(1+z^2/r^2)^{3/2}}{z}. \tag{17}$$

In Takahara et al. (1989), the left-hand side was ignored (see the Appendix).

Equation (17) can easily be integrated to give

$$-\frac{r_e}{z} + \frac{(r^2+z^2)^{1/2}}{z} + \frac{z}{(r^2+z^2)^{1/2}} = \chi \text{ (constant)}, \tag{18}$$

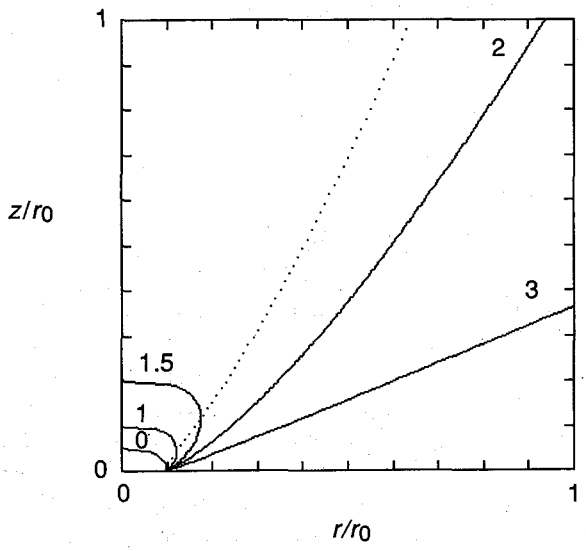

Fig. 1. Configuration of streamlines determined by the balance between the gravitational force and the centrifugal force perpendicular to the streamline. According to the values of χ indicated on each curve, several configurations are possible. We consider the case $\chi = 2$ in this paper as an example, since for $\chi \geq 2$ the streamlines extend to infinity. The dotted curve represents a configuration in which dr/dz is dropped in the determination (see the Appendix).

or written as an explicit form of $r = r(z; r_e)$:

$$r^2 = \left\{ \frac{r_e + \chi z + [(r_e + \chi z)^2 - 4z^2]^{1/2}}{2} \right\}^2 - z^2. \tag{19}$$

The configuration of the streamlines forms a one-parameter family through χ. This integration constant, χ, corresponds to the direction in which the gas is initially ejected from the disk surface.

In figure 1, several streamline configurations in the meridional plane are shown by solid curves. The location of the flow base is fixed at $r_e = 1$. For a comparison, the streamline where dr/dz is neglected is also shown by a dotted curve (see the Appendix).

It should be noted that the family of the configuration of streamlines shown in figure 1 is just the coordinate orthgonal to the equi-potential surfaces of the effective potential (11) under a constant specific angular momentum (6). Therefore, the combined gravitational and centrifugal forces always act backward along the streamline. The gas is thus driven by the pressure gradient force along the streamline. The dotted curve, on the other hand, is the locus of the points where the radial derivative of the effective potential vanishes.

The cross-sectional area (8) along the streamline is explicitly written as

$$A = \left[1 + \left(\frac{dr}{dz}\right)^2\right]^{-1/2} \frac{\{r_e + \chi z + [(r_e + \chi z)^2 - 4z^2]^{1/2}\}^2}{4r_e[(r_e + \chi z)^2 - 4z^2]^{1/2}}, \tag{20}$$

where dr/dz is given by equation (17).

As shown in figure 1, the streamlines are curved toward the rotation axis for $\chi < 2$. Since the gas cannot approach the vicinity of the rotation axis, due to the angular momentum barrier, streamlines with $\chi < 2$ are inadequate, at least far above the equator. Furthermore, in the case $\chi < 2$, the cross-sectional area decreases along the streamline.

On the other hand, for $\chi \geq 2$ the streamlines extend to infinity and the cross-sectional area increases along the streamline. We thus adopt the case $\chi \geq 2$ as the configuration of streamlines. In particular, we consider the case $\chi = 2$ in the next section.

4. The Global Pattern of Disk Winds

Now we examine the hydrodynamical winds from a geometrically thin disk, concentrating attention on the two-dimensional global properties, such as whether the gas can escape or not.

Since for the winds the sound speed c tends to zero at infinity, from the Bernoulli equation (16), the terminal speed v_∞ of the flow is expressed as

$$\frac{v_\infty^2}{2} = \frac{\gamma\varepsilon}{\gamma - 1}\frac{1}{r_e^q} - \frac{1}{2r_e}. \tag{21}$$

If the right-hand side of equation (21) is negative, the gas is gravitationally bound, as was pointed out in Paper I, where the rotation was not included and, therefore, the factor 1/2 on the right-hand side of equation (21) was dropped. On the other hand, the gas can escape to infinity for a positive value of the right-hand side.

Such global properties of disk winds depend on γ, the ratio ε, the radial position r_e of the wind base and, further, the temperature distribution q on the wind base. Hence, in the following of this section, we consider in turn such disk winds for several cases of the temperature distribution at the wind base; flatter case ($q < 1$), intermediate one ($q = 1$), and steeper one ($q > 1$). In addition, we set $\chi = 2$ for the configuration of streamlines (as was stated). The results described below are qualitatively the same for the case $\chi \geq 2$, where the streamlines extend to infinity.

4.1. Case of $q < 1$

We first consider the case where the distribution of the enthalpy (or the temperature) at the wind base is flat. In the case $q < 1$, from equation (21), the gas is gravitationally bound when $r_e < [(\gamma - 1)/(2\gamma\varepsilon)]^{1/(1-q)}$, while it can escape to infinity otherwise. This situation is also seen below, regarding the locus of the critical points.

The positions of critical point, z_c (or r_c), in each streamline (specified by r_e) are determined by the condition that the numerator of equation (13) vanishes: $N = 0$. In the upper panel of figure 2, the loci of critical points z_c are plotted as a function of r_e

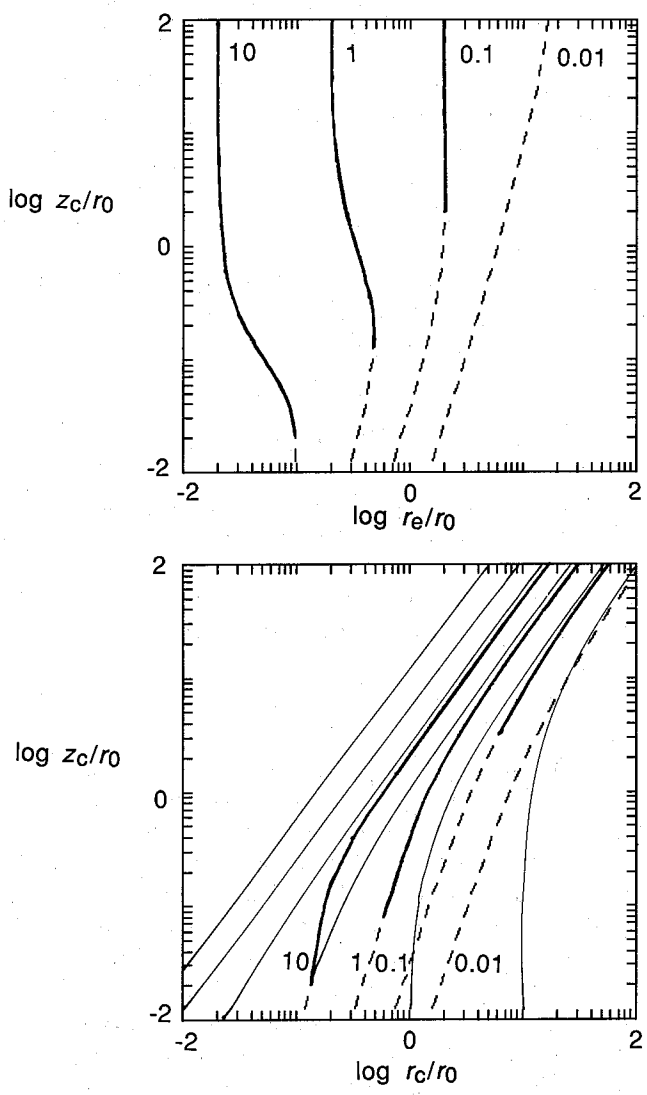

Fig. 2. Loci of critical points z_c for various values of ε in the case of a flatter temperature distribution ($q = 0$). The values of ε are indicated on each curve. The parameter γ is fixed as $\gamma = 5/3$. In the upper panel, z_c is plotted as a function of r_e, the position of the flow base on the equator, whereas the relations between r_c and z_c are displayed in the lower panel. The solid curves indicate the critical points of the saddle type, while critical points of the center type are denoted by dashed curves. Note that in some range of r_e there are multiple critical points. Moreover, inside $r_e < [(\gamma - 1)/(2\gamma\varepsilon)]^{1/(1-q)}$, there are no wind solutions. Thin solid curves in the lower panel represent the streamlines adopted.

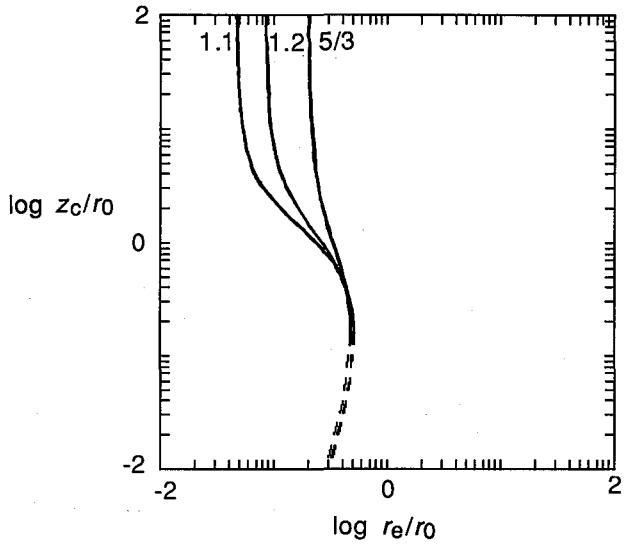

Fig. 3. Loci of critical points z_c for various values of γ in the case of $q = 0$. Parameter ε is fixed as $\varepsilon = 1$.

for various values of ε in the typical case of $q = 0$ and $\gamma = 5/3$. In the lower panel of figure 2, on the other hand, the relations between r_c and z_c in the meridional plane are plotted by thick solid curves. These curves represent the sonic surfaces of the flow field for a given set of parameters. The configuration of the streamlines is expressed by thin solid curves.

As mentioned above, in the inner region ($r_e < 0.2\ \varepsilon$ for figure 2), there are no wind solutions extending to infinity and the gas near the disk plane is gravitationally bound to form a corona, since for the given parameters the thermal energy of gas at the flow base is too small for the gas to be lifted up to infinity. Whereas, in the outer region, the gas can flow out from the disk to infinity, either as a supersonic wind passing through critical points or as a supersonic wind (or a subsonic breeze) without passing through them. These global properties are qualitatively the same as those demonstrated in Paper I. In addition, it is also found that multiple critical points on the same streamline appear in some range for the present case. The solid (dashed) curves represent the saddle (center) type in figure 2.

Since the critical solutions of each streamline are similar to those in Paper I, we do not present them here.

The dependence of the positions of the critical points on γ is shown in figure 3. Parameter ε is fixed as $\varepsilon = 1$. As expected, the wind region extends inward as γ approaches unity.

4.2. Case of $q = 1$

We next consider the case where the temperature at the wind base decreases as $1/r_e$. In this case, the gas is free (bound) all over the disk when ε is greater (less)

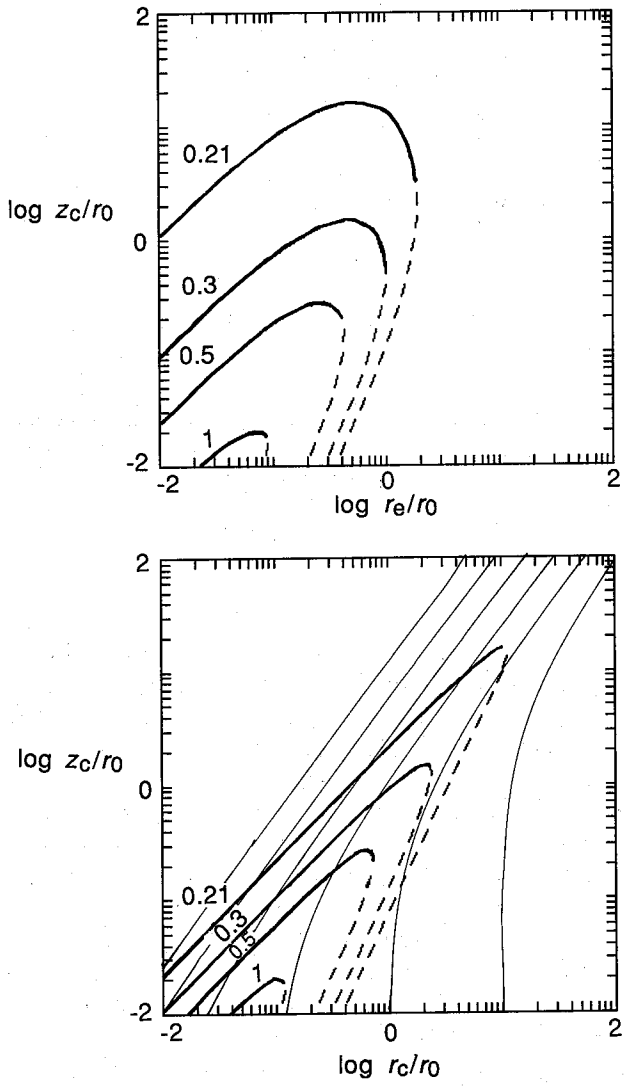

Fig. 4. Same as figure 2, but for the case in which the temperature at the flow base varies as $1/r_e$ ($\gamma = 5/3$). Note that the loci of critical points are closed.

than $(\gamma - 1)/(2\gamma)$.

The loci of critical points are plotted as a function of r_e for various values of ε in the upper panel of figure 4. Parameter γ is fixed as $\gamma = 5/3$. In the lower panel, the transonic surfaces in the meridional plane are shown.

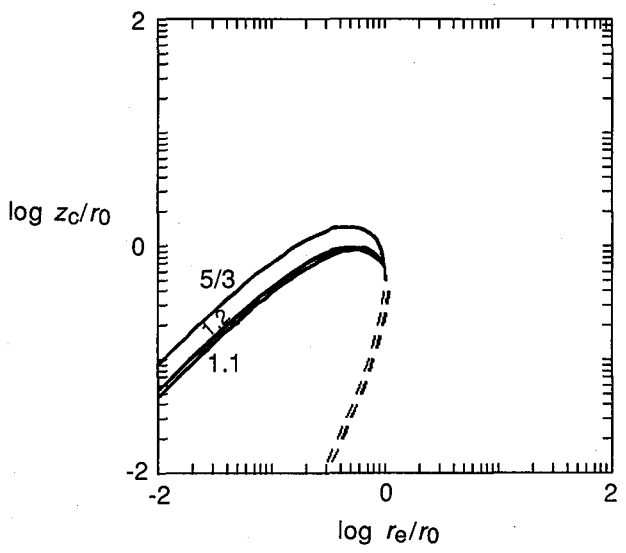

Fig. 5. Same as figure 3, but for the case in which the temperature at the wind base varies as $1/r_e$ ($\varepsilon = 0.3$).

Unlike the case of a flatter temperature distribution, $q < 1$, the locus is not open but closed for $\varepsilon > (\gamma - 1)/(2\gamma)$. If the gas escapes to infinity, it then flows as a transonic wind from the inner region, while acting like an initially supersonic wind or subsonic breeze from the outer region.

The γ-dependence is shown in figure 5 for the case of $\varepsilon = 0.3$. The global properties of the flow in the case of $q = 0$ does not strongly depend on γ.

4.3. Case of $q > 1$

Finally, we show the results of a steeper temperature distribution. In the inner region of $r_e < [2\varepsilon\gamma/(\gamma - 1)]^{1/(q-1)}$, the gas can escape, while being bound in the outer disk.

The loci of critical points in the case $q = 2$ and $\gamma = 5/3$ are plotted for various values of ε in the upper panel of figure 6. In the lower panel, the transonic surfaces in the meridional plane are shown. In the inner wind region, the position of the critical points moves to infinity as the flow base approaches the outer corona region.

The dependence on γ is shown in figure 7. In this case, the inner wind region extends outward as γ approaches unity.

5. Discussion

In this paper we examine the global properties of thermal disk winds under an approximation in which the configuration of the streamlines is determined by the balance between the gravitational force by the central object and the centrifugal force

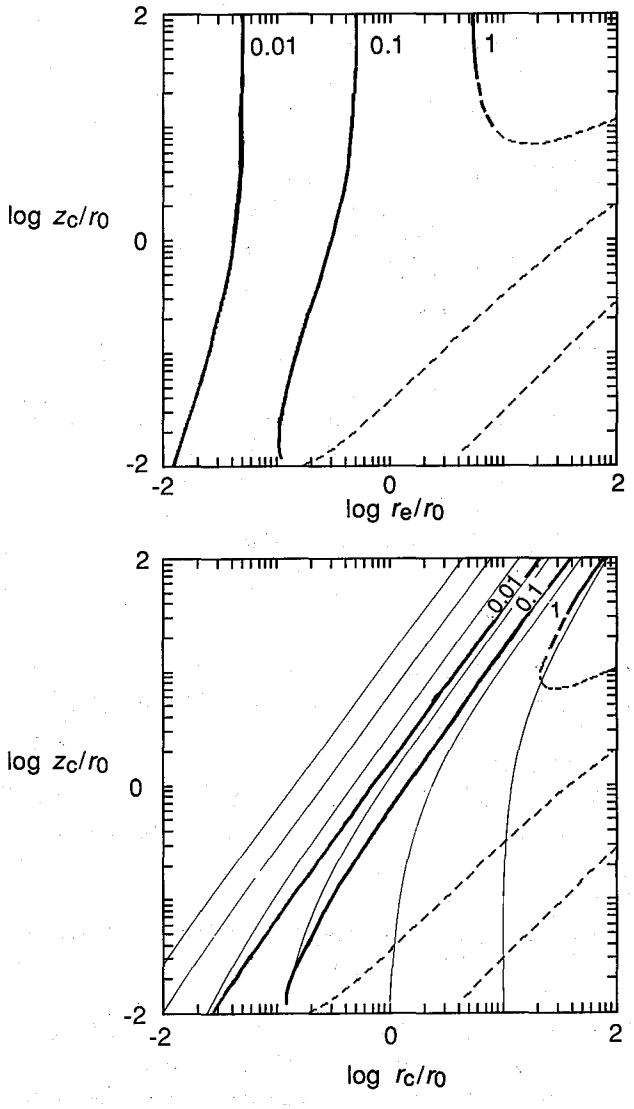

Fig. 6. Same as figure 2, but with a steeper temperature distribution of $q = 2$ ($\gamma = 5/3$). In this case, the gas in the inner region escapes while being bound in the outer region. Furthermore, in the inner wind region, there appear multiple critical points, while the critical points appearing in the outer corona region are of the center type.

perpendicular to the streamline, itself. We demonstrate a two-dimensional pattern, similar to the results of Paper I in which the rotation was not included. That is, when the temperature distribution at the wind base on the surface of the disk is flatter (than

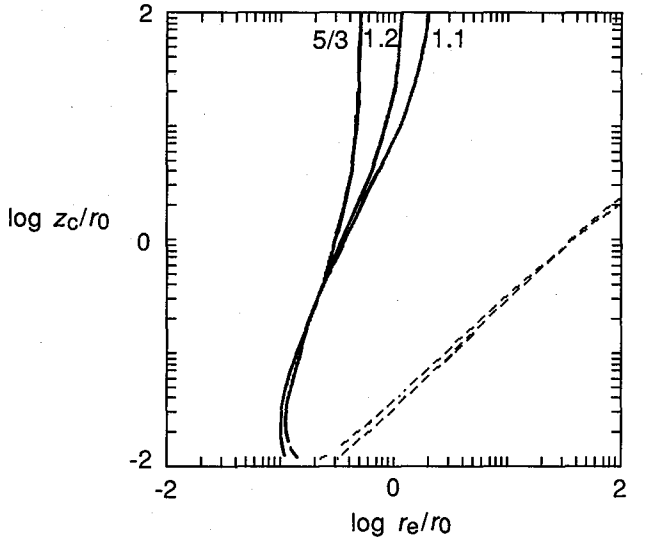

Fig. 7. Same as figure 3, but with a steeper temperature distribution of $q = 2$ ($\varepsilon = 1$).

$1/r_e$), the gas on the inner region of the disk is gravitationally bound to form a corona (figures 2 and 3). However, the gas in the outer region can escape to infinity. Hence, hollow cylindrical winds may be realized. In the inner wind region, the terminal speed of the winds are given by equation (21) from energy conservation along the streamline.

On the other hand, if the temperature at the wind base changes as $1/r_e$, the terminal speed becomes $v_\infty^2/2 = [\gamma\varepsilon/(\gamma-1) - 1/2]/r_e$. In this case, the entire region of the disk surface is windy or bound (figure 4). If it is windy, the terminal speed is greater in the inner region.

Finally, for a steeper temperature distribution (than $1/r_e$), the situation is reversed: that is, the gas in the inner disk can escape while the gas in the outer region is bound (figures 5 and 6). Moreover, disk winds may become filling-up winds.

In the present disk winds, multiple critical points also appear, as in Paper I. A multiplicity of critical points often arises by the effects of rotation (Limber 1967; Henriksen and Heaton 1975; Fukue 1987), variable cross-section (Kopp and Holzer 1976), or an additional gravitating body (Fukue and Yamamoto 1986). In the present case, the multiplicity occurs due to a deviation in the shape of the gravitational potential along the streamline from that of a spherical wind, as in the case of Paper I; the effect of rotation is not essential.

In this paper, we do not consider the configurations of streamlines with $\chi < 2$ in figure 1, since in such cases the streamlines converge toward the rotation axis. However, in the vicinity of the disk, there is no preferred direction for the gas to start. If the gas starts from the disk surface in the vertical direction ($\chi = 0$), it is naturally curved toward the rotation axis and *self-collimated* under the actions of

gravity and rotation. If such a self-collimation really takes place in the disk winds, the gas encounters an angular momentum barrier and may again turn to a diversing flow along the barrier. For such a stage, of course, the pressure gradient force cannot be ignored in the force balance perpendicular to the streamline, and the present treatment would be violated. Numerical simulations are therefore necessary.

The pressure gradient term perpendicular to the streamline also becomes significant near the disk surface when the temperature gradient along the disk plane is so steep. Hence, the streamline for $q \gtrsim 1$ is somewhat modified for a more realistic flow. For a uniform temperature distribution of $q \sim 0$, however, this pressure gradient term perpendicular to the streamline can be safely ignored. Exactly speaking, in the left-hand side of equation (1), there is an inertial term that arises from the centrifugal force due to the curvature of the streamline in the meridional plane. We have also dropped that term since, for a streamline of $\chi > 2$, the curvature of the streamline is small.

Various mechanisms are supposed to drive thermal disk winds, the most important of which are the irradiation of the accretion disk by the central source (Hayakawa 1981; Hoshi 1984) and the two-temperature hot accretion disk (Shapiro et al. 1976; Kusunose and Takahara 1988; White and Lightman 1989). In the former case, the irradiation is dominant in the outer disk, where the disk temperature varies as $T \propto r^{-3/7}$ (Hayakawa 1981). If the temperature of the wind base is proportional to the disk temperature, the temperature distribution is rather flat and the disk winds may flow in the outer region of the irradiation disk.

In hot accretion disks, the gas is heated to a relativistic temperature in the inner region of the accretion disk. In particular, if pair processes are taken into consideration, no steady solutions of a hot accretion disk have been found in the region around $5r_{\rm g}$, $r_{\rm g}$ being the Schwarzschild radius of the central object (Kusunose and Takahara 1988; White and Lightman 1989). Due to the pair creation processes, the electron temperature reaches a ceiling of $\sim 10^{10}$K in these regions (Kusunose and Takahara 1988). It thus seems that the temperature distribution is uniform ($q \sim 0$) there. Furthermore, if we set $T_0 = 10^{10}$K at $r_0 = 5r_{\rm g}$, we have $\varepsilon = 0.02$. Hence, from figures 2 and 3, the entire hot region around $5r_{\rm g}$ becomes windy for smaller γ, while only the outer part is windy for $\gamma \sim 5/3$. In the latter case, the inner part may initially puff up to form a geometrically thick disk; then, the pair winds start to blow from the surface of the thick disk where the depth of the gravitational potential is shallow.

The magnetic field of gas has not yet been taken into consideration. If the magnetic field is considered, Alfvénic critical points appear in addition to those of acoustic origin (Weber and Davis 1967; Blandford and Payne 1982; Sakurai 1987). Moreover, magnetic tension will affect the configuration of the streamlines. A study of the influence of the magnetic field on the disk is left as future work.

The authors would like to thank Professor S. Kato and Drs. S. Inagaki and Y. D. Tanaka for their useful comments. This work was supported in part by a Grant-in-Aid for Encouragement of Young Scientists of the Ministry of Education, Science and Culture (63740133, 01740144).

Appendix. The Case of Quasi-Vertical Streamlines

In Takahara et al. (1989), the term dr/dz is dropped in equation (17), although it is retained in the other equation (5) expressing the force along the streamline or in equation (8) for the cross-sectional area. By setting $dr/dz = 0$ in equation (17), the streamline becomes

$$z = r[(r/r_e)^{2/3} - 1]^{1/2}. \tag{A1}$$

This configuration is shown in figure 1 by a dotted curve. In this appendix, we briefly examine the hydrodynamical winds under the streamlines given by equation (A1) for a comparison, although our attention is concentrated on the two-dimensional global properties.

Under the configuration of streamlines (A1), the cross-sectional area yields

$$A = \frac{(r/r_e)^{7/3}}{[16(r/r_e)^{2/3} - 15]^{1/2}}. \tag{A2}$$

This cross-sectional area is not a monotonically increasing function of r (or z), but has a minimum at $r = r_e(35/32)^{3/2} \sim 1.14r_e$. That is, it initially decreases near the disk plane ($dA/dz < 0$); then, beyond $z > r_e(3/32)^{1/2}(35/32)^{3/2} \sim 0.350r_e$ it increases ($dA/dz > 0$). Since the numerator N of equation (13) cannot vanish in the region where the cross-sectional area decreases, critical points always exist in the A-increasing region. As in the text, for parameters γ and ε, we seperately consider disk winds in the several cases of the temperature distribution at the wind base.

A.1. Case of $q < 1$

In the upper panel of figure A1, the loci of critical points z_c are plotted by the solid curves as a function of r_e in the typical case of $q = 0$ and $\gamma = 5/3$ for various values of ε. In the lower panel of figure A1, on the other hand, the relations between r_c and z_c in the meridional plane is plotted by thick solid curves.

Inside $r_e < [(\gamma - 1)/(2\gamma\varepsilon)]^{1/(1-q)}$, the gas is gravitationally bound; however, it can escape in the outer region, similar to the case discussed in the text. In contrast to the case shown in figures 2 or 3, however, multiple critical points do not appear in this case. This means that the properties of the disk winds discussed in this appendix and by Takahara et al. (1989) resemble spherical winds, like solar winds. Furthermore, this shows that the transonic nature of disk winds near the disk plane depends naively on the configuration of the streamlines: that is, on the forms of the cross-sectional area $A(z)$ and the effective potential $\phi(z)$. As already stressed, however, the global behavior, such as whether the gas can escape or not, is essentially independent of them. It depends mainly on the temperature distribution at the flow base.

It should be noted that the loci move self-similarly as a function of ε. Such a self-similarity is lost in the case described in the text because of the integration constant χ.

As already noted, the critical points are always located in the region $z > 0.350r_e$.

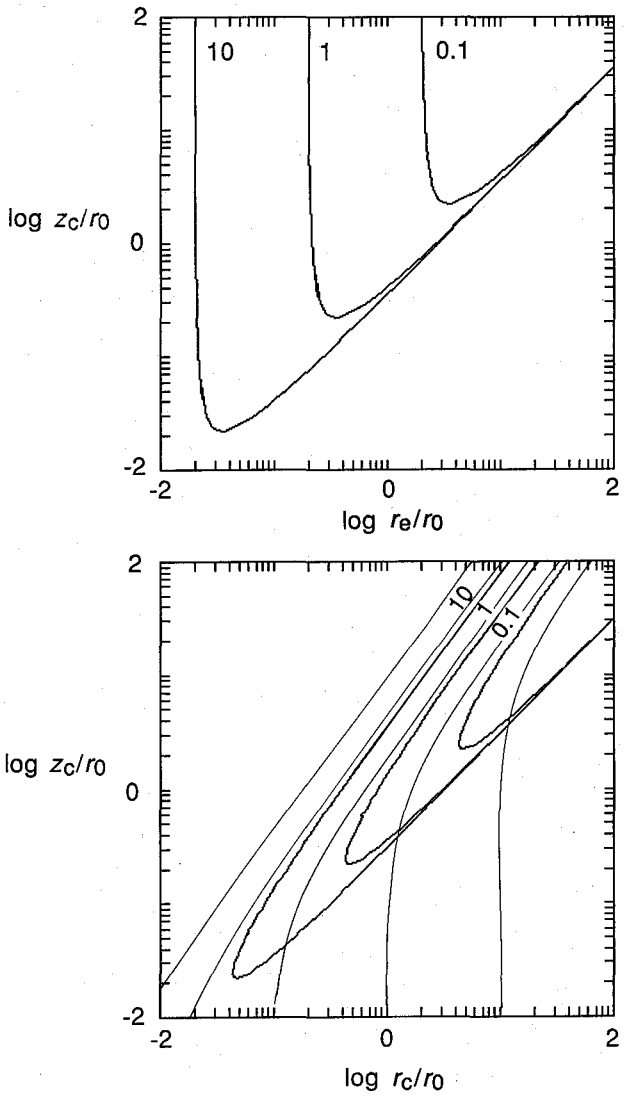

Fig. A1. Loci of critical points z_c for various values of ε in the case of a flatter temperature distribution ($q = 0$). The values of ε are indicated on each curve. Parameter γ is fixed as $\gamma = 5/3$. See the legend of figure 2. Since the configuration of the streamlines is different from that of figure 2, the locations of the critical points are changed. The global properties, however, do not depend on the streamlines.

A.2. Case of $q = 1$

The case where the temperature at the wind base decreases as $1/r_e$ is shown in figure A2 for various values of ε ($\gamma = 5/3$). The gas is free (bound) when ε is greater

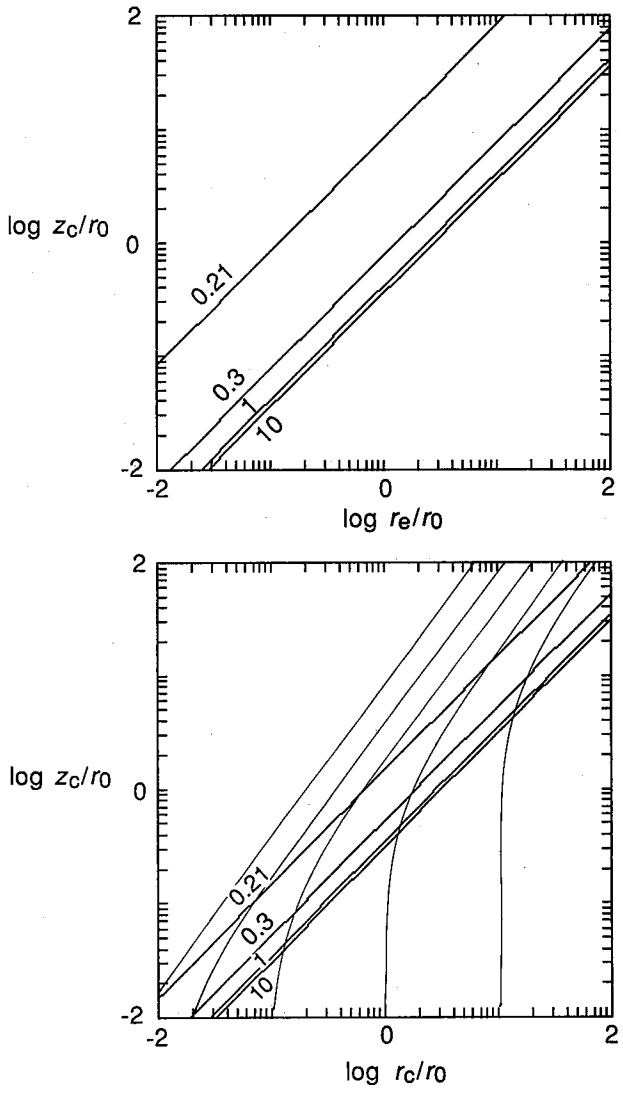

Fig. A2. Same as figure A1, but for the case in which the temperature at the flow base varies as $1/r_e$ ($\gamma = 5/3$). See also figure 4.

(less) than $(\gamma - 1)/(2\gamma)$.

In this case, the transonic surface becomes a cone whose top coincides with the center and, therefore, it intersects all of the streamlines. Furthermore, the global flow pattern becomes self-similar.

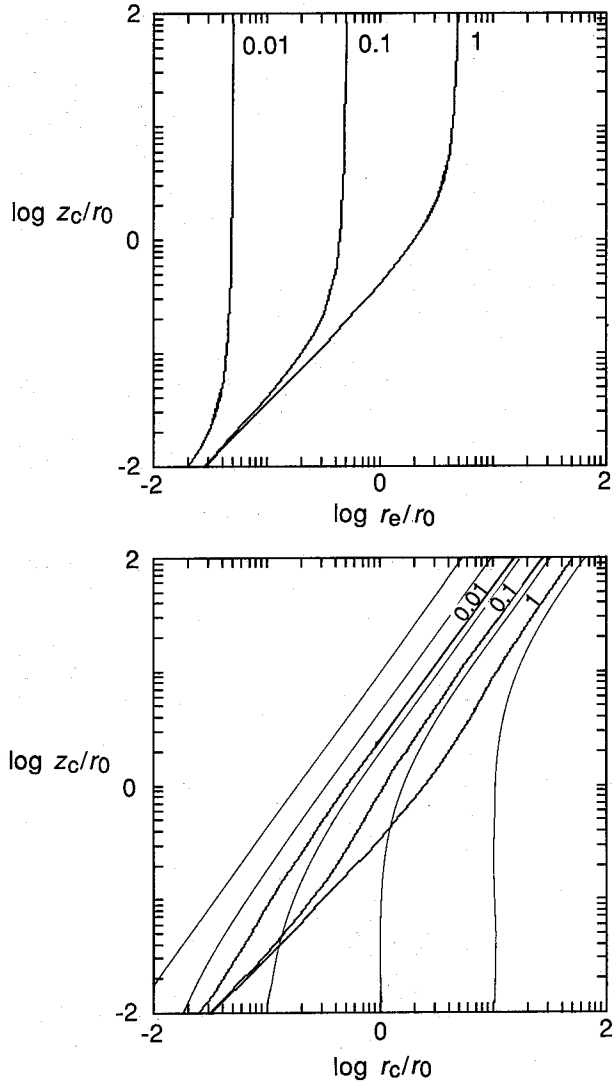

Fig. A3. Same as figure A1, but with a steeper temperature distribution of $q = 2$ ($\gamma = 5/3$). See also figure 6.

A.3. Case of $q > 1$

Finally, we show the results of a steeper temperature distribution ($q = 2$) in figure A3 for various values of ε ($\gamma = 5/3$). In the inner region of $r_e < [2\gamma\varepsilon/(\gamma - 1)]^{1/(q-1)}$, the gas can escape, while it is bound in the outer disk.

References

Begelman, M. C., and McKee, C. F. 1983, *Astrophys. J.*, **271**, 89.
Begelman, M. C., McKee, C. F., and Shields, G. A. 1983, *Astrophys. J.*, **271**, 70.
Blandford, R. D., and Payne, D. G. 1982, *Monthly Notices Roy. Astron. Soc.*, **199**, 883.
Calvani, M., and Nobili, L. 1983, in *Astrophysical Jets*, ed. A. Ferrari and A. G. Pacholczyk (Reidel, Dordrecht), p. 189.
Chakrabarti, S. K. 1986, *Astrophys. J.*, **303**, 582.
Eggum, G. E., Coroniti, F. V., and Katz, J. I. 1985, *Astrophys. J. Letters*, **298**, L41.
Ferrari, A., Habbal, S. R., Rosner, R., and Tsinganos, K. 1984, *Astrophys. J. Letters*, **277**, L35.
Fukue, J. 1982, *Publ. Astron. Soc. Japan*, **34**, 163.
Fukue, J. 1983, *Publ. Astron. Soc. Japan*, **35**, 539.
Fukue, J. 1987, *Publ. Astron. Soc. Japan*, **39**, 309.
Fukue, J. 1989, *Publ. Astron. Soc. Japan*, **41**, 123 (Paper I).
Fukue, J., and Yamamoto, S. 1986, *Publ. Astron. Soc. Japan*, **38**, 895.
Hayakawa, S. 1981, *Publ. Astron. Soc. Japan*, **33**, 365.
Henriksen, R. N., and Heaton, K. C. 1975, *Monthly Notices Roy. Astron. Soc.*, **171**, 27.
Hoshi, R. 1984, *Publ. Astron. Soc. Japan*, **36**, 785.
Katz, J. I. 1980, *Astrophys. J. Letters*, **236**, L127.
Kopp, R. A., and Holzer, T. E. 1976, *Solar Phys.*, **49**, 43.
Kusunose, M., and Takahara, F. 1988, *Publ. Astron. Soc. Japan*, **40**, 435.
Limber, D. N. 1967, *Astrophys. J.*, **148**, 141.
Lu, J. F. 1986, *Astron. Astrophys.*, **168**, 346.
Lynden-Bell, D. 1969, *Nature*, **223**, 690.
Meier, D. L. 1979, *Astrophys. J.*, **233**, 664.
Meier, D. L. 1982, *Astrophys. J.*, **256**, 681.
Sakurai, T. 1987, *Publ. Astron. Soc. Japan*, **39**, 821.
Shapiro, S. L., Lightman, A. P., and Eardley, D. M. 1976, *Astrophys. J.*, **204**, 187.
Takahara, F., Rosner, R., and Kusunose, M. 1989, *Astrophys. J.*, **346**, 122.
Weber, E. J., and Davis, L., Jr. 1967, *Astrophys. J.*, **148**, 217.
White, T. R., and Lightman, A. P. 1989, *Astrophys. J.*, **340**, 1024.